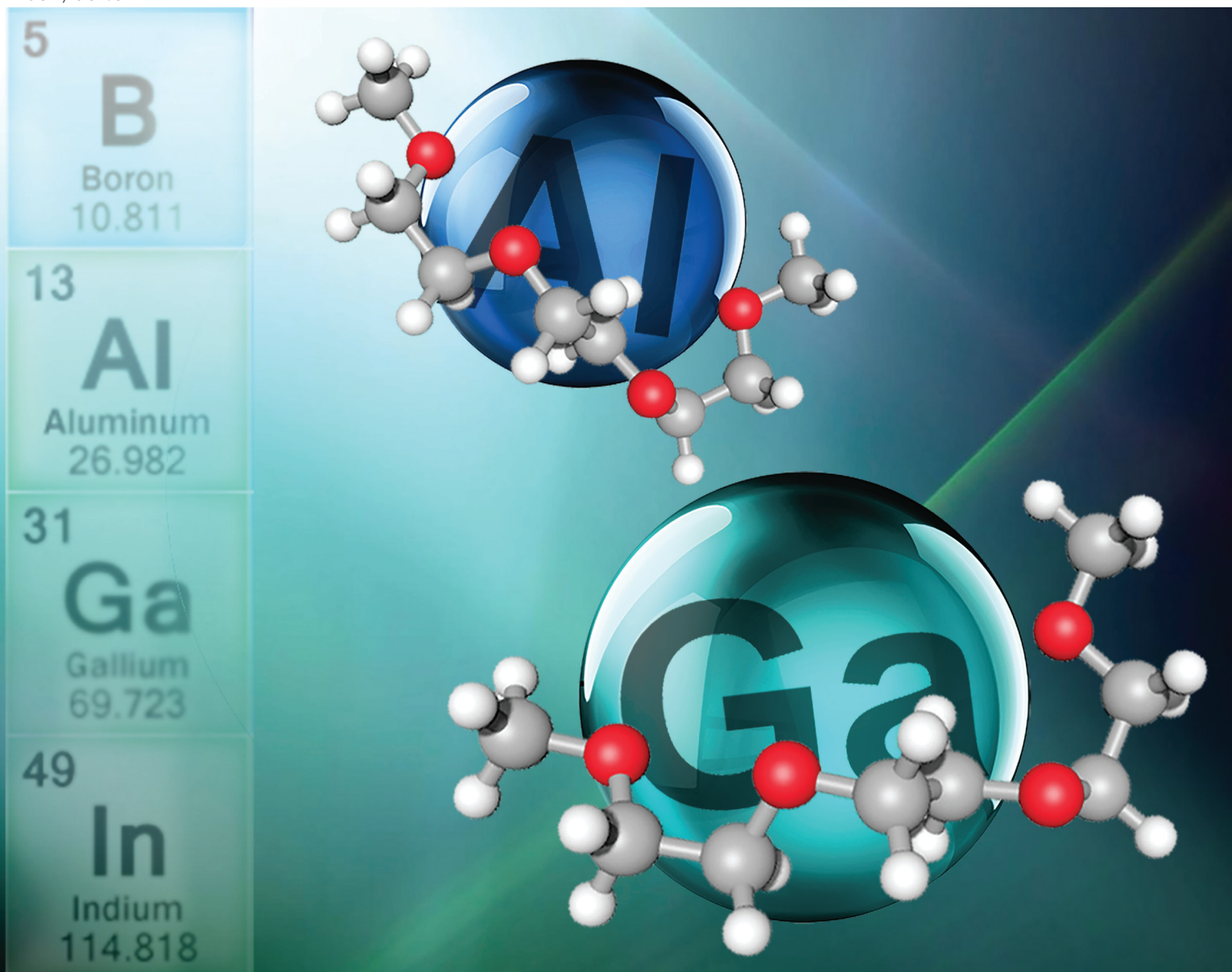


Dalton Transactions

An international journal of inorganic chemistry

rsc.li/dalton



ISSN 1477-9226

PAPER

Małgorzata Swadźba-Kwaśny, Anna Chrobok *et al.*
Al(III) and Ga(III) triflate complexes as solvate ionic liquids:
speciation and application as soluble and recyclable Lewis
acidic catalysts

PAPER

[View Article Online](#)
[View Journal](#) | [View Issue](#)Cite this: *Dalton Trans.*, 2024, **53**, 19143

Al(III) and Ga(III) triflate complexes as solvate ionic liquids: speciation and application as soluble and recyclable Lewis acidic catalysts†

Justyna Więclawik,^a Alina Brzęczek-Szafran,^a Sebastian Jurczyk,^b Karolina Matuszek,^c Małgorzata Swadźba-Kwaśny^d and Anna Chrobok^{*d}

This work reports on the first solvate ionic liquids (SILs) based on aluminium(III) and gallium(III) triflates, M(OTf)₃, and triglyme (G3). Liquid-phase speciation of these new SILs was studied by multinuclear NMR spectroscopy. Across the compositional range of G3 : M(OTf)₃ mixtures, both metals were found to be in a hexacoordinate environment, with both G3 and [OTf][−] ligands present in the first coordination sphere, and apparently exchanging through a dynamic equilibrium. The Lewis acidity was quantified by the Gutmann acceptor number (AN) and compared to the performance of SILs as Lewis acidic catalysts in model [3 + 3] cycloadditions. Despite saturated coordination, AN values were relatively high, reaching AN = ca. 71–83 for Al-SILs and ca. 80–93 for Ga-SILs, corroborating the labile nature of the metal–ligand bonding. In a model catalytic reaction, SILs were fully soluble in the reaction mixtures, in contrast to the corresponding triflate salts. The catalytic performance of SILs exceeded that of the corresponding triflate salts, and Ga-SILs were more active than Al-SILs, in agreement with AN measurements. In conclusion, the new Group 13 SILs can be considered as soluble and catalytically active forms of their corresponding metal triflates, with potential uses in catalysis.

Received 14th August 2024,
Accepted 3rd October 2024

DOI: 10.1039/d4dt02314e

rsc.li/dalton

Introduction

The concept of functional liquids, in which a metal cation was solvated by L-type ligands, was first introduced by Angell in 1965.¹ He described hydrates, such as Ca(NO₃)₂·4H₂O, as a “new class of molten salt mixtures”, recognising that solvating the metal cation generates low-melting hydrates with high conductivities, potentially useful as electrolytes.² In contrast to molten salts, however, the thermal stability of such “molten salt mixtures” was limited by the aqua ligand.

A similar approach was used in the design of liquid coordination complexes (LCCs), in which metal halides were combined with sub-equimolar quantities of organic L-donors, e.g.

AlCl₃ and acetamide, or GaCl₃ and trioctylphosphine oxide.^{3,4} LCCs (Fig. 1b), developed as less expensive and more tuneable alternatives to chlorometallate ionic liquids (Fig. 1a), were subsequently demonstrated to be Lewis acidic catalysts in an array of reactions: oligomerisation of olefins,⁵ Diels–Alder cycloaddition,⁴ and Friedel–Crafts alkylation,⁶ as well as co-catalysts in heterogeneous catalysis through solid catalysts with ionic liquid layer (SCILL).⁷ However, most reported LCCs, like conventional chlorometallate ionic liquids, are highly corrosive due to their high chloride content.

Salts of Lewis acidic metals (M = Al, Ga, and Ln) and trifluoromethanesulfonic acid (known as triflates, OTf) are stable in aqueous media, chloride-free and catalytically active at low concentrations.^{8,9} However, they suffer from poor solubility in most solvents.^{10,11} In an attempt to enhance their solubility, we have developed triflometallate ionic liquids, synthesised by the reaction of triflate ionic liquids and Group 13 triflates (Fig. 1c).¹² While catalytically active, these ILs are extremely viscous and very expensive. Seeking further alternatives, we have decided to explore the concept of solvate ionic liquids (SILs).

Watanabe and co-workers developed SILs,^{13–16} exemplified by equimolar mixtures of Li[NTf₂] and triglyme (G3), or tetraglyme (G4), for energy storage applications (Fig. 1d). Mandai *et al.*¹⁴ provided formalised criteria for “good” SILs, which

^aDepartment of Organic Chemical Technology and Petrochemistry, Faculty of Chemistry, Silesian University of Technology, Bolesława Krzywoustego 4, 44-100 Gliwice, Poland. E-mail: anna.chrobok@polsl.pl

^bInstitute for Engineering of Polymer Materials and Dyes, Lukasiewicz Research Network, Skłodowskiej-Curie 55, PL-87100 Toruń, Poland

^cAddress School of Chemistry, Monash University, Clayton, Victoria 3800, Australia

^dThe QUILL Research Centre, School of Chemistry and Chemical Engineering, Queen's University of Belfast, David Keir Building, Stranmillis Road, Belfast BT9 5AG, UK. E-mail: m.swadzba-kwasny@qub.ac.uk

†Electronic supplementary information (ESI) available: Referenced data S1 and S2, detailed experimental information and TGA thermal curves. See DOI: <https://doi.org/10.1039/d4dt02314e>

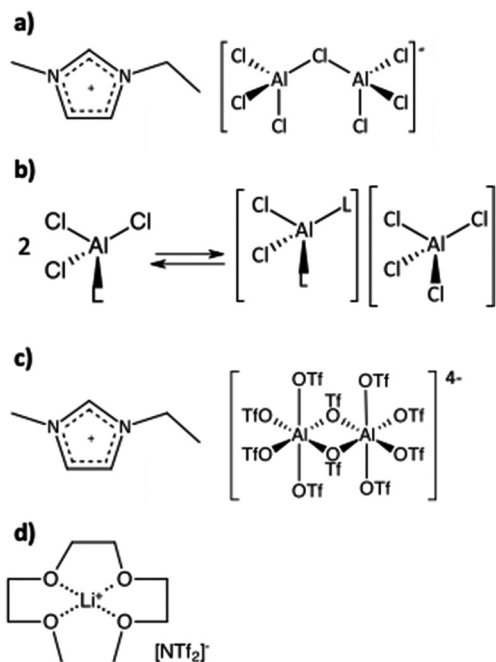


Fig. 1 Examples of the structures of metal-containing ionic liquids: (a) chlorometallate ionic liquid, (b) liquid coordination complex (LCC),³ (c) trifluoroaluminate ionic liquid,⁸ and (d) solvate ionic liquid.¹⁴

behave like ionic liquids, not like solutions of salts in molecular solvents (they are solvent-in-salt systems, not salt-in-solvent). Such SILs combine flexible polydentate ligands, solvating a Group 1 or 2 metal, and weakly basic anions, such as bis(trifluoromethanesulfonate)imide, $[\text{NTf}_2]^-$. This design yields long-lived robust cations: alkali metals solvated by glyme. “Good” SILs are relatively simple to synthesise, thermally stable, electrically conductive and non-flammable, and therefore make very good electrolytes.^{17–24}

Since SILs have been developed in the context of energy storage applications, their uses in catalysis are scarce.²⁵ Eyckens *et al.* used SILs in Diels–Alder and $[2 + 2]$ cycloadditions, reporting that higher yields (up to 94%) and improved reaction safety can be achieved by replacing a solution of lithium salt in a molecular solvent with $[\text{Li}(\text{G3})][\text{NTf}_2]$ or $[\text{Li}(\text{G4})][\text{NTf}_2]$, in the formation of oxetanone.²⁶ Obregón-Zúñiga *et al.* found improved yield and selectivity in an asymmetric aldol reaction in the presence of SILs, also $[\text{Li}(\text{G3})][\text{NTf}_2]$ or $[\text{Li}(\text{G4})][\text{NTf}_2]$, due to their involvement in the catalytically active supramolecular aggregate formation.²⁷ Other uses include Kabachnik–Fields reactions,²⁸ stereo- and regioselective ring opening of epoxides,²⁹ and catalytic additives for curing epoxy systems.³⁰ Importantly for this work, all catalytic studies to date have been focussed on Li-based SILs, a weak Lewis acid. Although SILs based on Na, K, Mg and Al are known, they have only been used in energy storage applications.^{31,32}

In this contribution, we combined our expertise in the design and study of Lewis acidic LCCs and ILs with the potential offered by the solvate ionic liquid design to report a series of solvate ionic liquids based on triflate salts of aluminium

and gallium and triglyme (G3). We delved into the speciation of these materials using multinuclear NMR spectroscopy and probed their acidity with the Gutmann acceptor number (AN). Our investigation revealed intricate speciation patterns and strong Lewis acidity of these new Group 13 SILs, demonstrated directly through a catalytic application in a model $[3 + 3]$ cycloaddition reaction. The study highlights notable differences in the coordination chemistry and Lewis acidity of Al-SILs and Ga-SILs, providing new insights into the chemistry of Group 13 metals.

Experimental

Materials

Aluminium(III) trifluoromethanesulfonate (99.9%), triethylene glycol dimethyl ether (99%), triethylphosphine oxide (97%), decane (99%), isoprene (99%, contains <1000 ppm *p*-tert-butylcatechol as an inhibitor), 2.0 M trimethylaluminum solution in toluene, and anhydrous toluene (99.8%) were all purchased from Sigma Aldrich and used as received. Phosphoric(v) acid (85% in D_2O) was also purchased from Sigma Aldrich. 2,4-Dimethylphenol (99%) and gallium(III) trifluoromethanesulfonate (99%) were purchased from Thermo Fisher Scientific. The synthesis of $\text{Al}(\text{NTf}_2)_3$ is described in the ESI.†

General procedure for the synthesis of SILs

The SILs were synthesized in a glovebox under an inert argon atmosphere (<0.6 ppm O_2 and H_2O). The triglyme (G3) and appropriate metal salt $\text{M}(\text{OTf})_3$ ($\text{Al}(\text{OTf})_3$ or $\text{Ga}(\text{OTf})_3$) were weighed into a vial at various molar ratios from 2 : 1 to 10 : 1 ($\chi_{\text{M}(\text{OTf})_3} = 0.09\text{--}0.33$). The mixture was allowed to react in a glovebox (40–45 °C, 3 h), and then the heat was turned off and the mixture was further stirred overnight.

The same procedure was used for $\text{Al}(\text{NTf}_2)_3$ and G3, with $\chi_{\text{Al}(\text{NTf}_2)_3} = 0.09\text{--}0.50$.

Multinuclear NMR spectroscopy

All NMR spectra (^1H , ^{13}C , ^{19}F , ^{27}Al , ^{31}P and ^{71}Ga) were recorded using a Bruker Avance DPX 400 MHz spectrometer. All samples were studied at 297 K, neat using a $\text{DMSO}-d_6$ or D_2O filled, sealed capillary as an external lock. In the case of ^{27}Al NMR, a solution of $\text{Al}(\text{NO}_3)_3$ hydrate in D_2O was used as an external reference. In ^{71}Ga NMR spectroscopy, a solution of $\text{Ga}(\text{NO}_3)_3$ hydrate in D_2O was used as an external reference and in ^{19}F NMR, fluorobenzene in acetone- d_6 was used as an external reference.

Acceptor number determination

Every ionic liquid was sampled into three different NMR tubes, to which triethylphosphine oxide (TEPO) was added at the following concentrations: 1 wt%, 2 wt% and 3 wt%. An 85% phosphoric(v) acid solution in D_2O enclosed in a capillary was used as the external standard. After TEPO dissolved in the ionic liquid, the ^{31}P NMR spectra were recorded at room temperature and at 161.89 MHz using an Agilent 400 MHz spectro-



meter. The measured ^{31}P NMR chemical shift for each ionic liquid-TEPO concentration arrangement was extrapolated to infinite dilution of TEPO, δ_{inf} . The referential value was the TEPO chemical shift in hexane extrapolated to infinite dilution, $\delta_{\text{inf hex}} = 0$ ppm. For each ionic liquid, the acceptor number was calculated based on the formula: $\text{AN} = 2.348 \cdot \delta_{\text{inf}}$, as described in the literature.^{33,34}

General procedure for [3 + 3] cycloaddition

All reactions were carried out under a protective atmosphere of argon. The catalyst (1–5 mol% per 1.00 mol of isoprene) was placed in a flask. Then 0.98 g of 2,4-dimethylphenol (8 mmol) and 0.27 g of isoprene (4 mmol) were added along with 0.10 g (0.7 mmol) of decane as an internal standard. The reaction was carried out using a magnetic stirrer at various temperatures (20–40 °C). The progress of the reaction was monitored by gas chromatography. GC analysis was performed in anhydrous hexane stored over molecular sieves.

Results and discussion

Design of Group 13 SILs

Initial screening experiments included three Group 13 salts: aluminium trifluoromethanesulfonate, $\text{Al}(\text{OTf})_3$, gallium(III) trifluoromethanesulfonate, $\text{Ga}(\text{OTf})_3$, and aluminium bis(trifluoromethane)sulfonimide, $\text{Al}(\text{NTf}_2)_3$, combined with triethylene glycol dimethyl ether (triglyme, G3).

Considering that non-coordinating anions were reported to be the best candidates for generating “good” SILs, mixtures of $\text{Al}(\text{NTf}_2)_3$ and G3 were tested first. Combinations with high loadings of the metal salt, $\chi_{\text{Al}(\text{NTf}_2)_3} = 0.33$ and 0.51, where $\chi_{\text{Al}(\text{NTf}_2)_3}$ is the molar ratio of $\text{Al}(\text{NTf}_2)_3$, were homogeneous and extremely viscous liquids. Decreasing the molar fraction of $\text{Al}(\text{NTf}_2)_3$ resulted in apparent autocatalytic decomposition: the mixtures darkened and a dark-brown insoluble solid precipitated from the liquid glyme. This explained the lack of literature data on $\text{Al}(\text{NTf}_2)_3$ and glyme mixtures, while there are several papers on $\text{Al}(\text{OTf})_3$ and diglyme,^{35–37} and on AlCl_3 and glymes.^{38–40}

Subsequently, mixtures of $\text{G3}:\text{Al}(\text{OTf})_3$ and $\text{G3}:\text{Ga}(\text{OTf})_3$ were tested. Initially, it was anticipated that homogeneous compounds could be synthesised from equimolar reactant ratios, $\chi_{\text{M}(\text{OTf})_3} = 0.50$ (Fig. 2a). However, both $\text{G3}:\text{Al}(\text{OTf})_3$ and $\text{G3}:\text{Ga}(\text{OTf})_3$ systems formed homogeneous liquids from very low metal triflate loadings, up to $\chi_{\text{M}(\text{OTf})_3} = 0.33$, which is equivalent to two moles of G3 per mole of $\text{M}(\text{OTf})_3$. This suggested the possible formation of both ionic and charge-neutral complexes (exemplified in Fig. 2b), but also significantly more complex species, with either triflates or glymes acting as bridging ligands. Notably, while high metal concentrations ($\chi_{\text{M}(\text{OTf})_3} = 0.33, 0.25$) are expected to display SIL-like behaviour, low metal loadings ($\chi_{\text{M}(\text{OTf})_3} = 0.09, 0.10$, etc.) are expected to behave like solutions of metal salts in an organic solvent.

The apparent viscosity and yellow/orange colour of the formed SILs decreased with decreasing metal loading (Table 1).

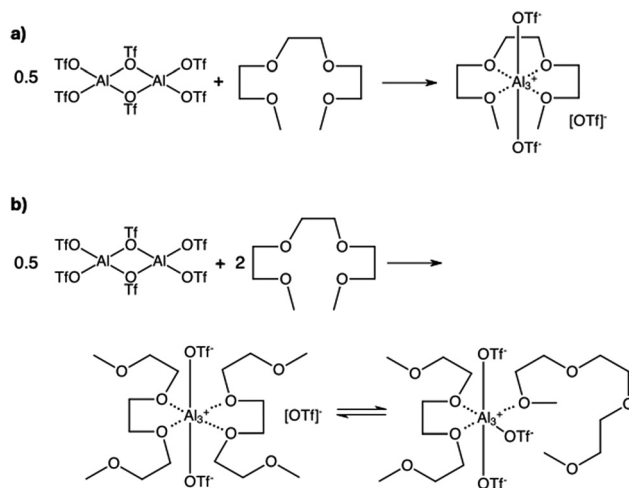


Fig. 2 Hypothetical speciation of Al-SILs synthesised at (a) $\chi_{\text{M}(\text{OTf})_3} = 0.50$ (reaction did not proceed to completion) and (b) $\chi_{\text{M}(\text{OTf})_3} = 0.33$ (reaction gave a homogeneous liquid).

Table 1 The composition, physical appearance and acceptor number (AN) values measured for the solutions and solvate ionic liquids in this study

Metal	$\chi_{\text{M}(\text{OTf})_3}$	G3 : $\text{M}(\text{OTf})_3$ molar ratio	Physical state	AN
Al	0.33	2 : 1	Very viscous, yellow liquid	70.9–82.7
	0.25	3 : 1	Viscous, light yellow liquid	70.8–82.7
	0.20	4 : 1	Pale yellow liquid	70.7–82.7
	0.17	5 : 1	Pale yellow liquid	70.7–82.6
	0.14	6 : 1	Pale yellow liquid	71.0–82.6
	0.13	7 : 1	Yellow hue liquid	71.4–82.6
	0.11	8 : 1	Yellow hue liquid	71.2–82.7
	0.10	9 : 1	Yellow hue liquid	71.1–82.5
	0.09	10 : 1	Yellow hue liquid	70.7–82.6
Ga	0.33	2 : 1	Very viscous, orange liquid	79.6–92.4
	0.25	3 : 1	Viscous, light orange liquid	81.6–92.3
	0.20	4 : 1	Pale orange liquid	80.4–92.3
	0.17	5 : 1	Pale orange liquid	80.3–93.4
	0.14	6 : 1	Pale orange liquid	80.3–92.8
	0.13	7 : 1	Orange hue liquid	79.9–92.6
	0.11	8 : 1	Orange hue liquid	79.6–93.4
	0.10	9 : 1	Orange hue liquid	80.0–93.5
	0.09	10 : 1	Orange hue liquid	80.1–93.3
—	—	1 : 0 (neat G3)	Colourless liquid	9.6

Acidity measurement with the Gutmann acceptor number

There are several scales currently used to measure Lewis acidity by different research groups; each relies on a probe that interacts with a Lewis acid, and experimental or computational methods are used to quantify the strength of the interaction. Computational methods have gained increasing popularity, but they require detailed information on the structure of the investigated species to accurately perform electronic structure computations and optimise the geometry (Global Electrophilicity Index – GEI)⁴¹ or evaluate enthalpy changes associated with fluoride/hydride coordination (Fluoride Ion



Affinity – FIA, and Hydride Ion Affinity – HIA).⁴² Spectroscopic methods, proposed by Gutmann and Childs, are based on NMR spectroscopic probes. They offer less fundamental insights, but they can be used without knowing the speciation, and in some cases, they were successfully used to corroborate speciation studies.^{43,44} Since the Gutmann acceptor number (AN) has been commonly used to measure the acidity of Lewis acidic ionic liquids,^{4,12,45} including solvate ionic liquids,²⁶ it has been selected for this study.

Following a standard procedure,^{4,12,33,34,46} AN values were determined from ³¹P NMR chemical shifts of an NMR probe, a weakly basic hard nucleophile, triethylphosphine oxide (TEPO). The probe was dissolved in G3 : M(OTf)₃ ionic liquids, across the available compositional range, $\chi_{M(OTf)_3} = 0.09$ –0.33.

In all cases, there were several distinguishable signals, situated within a narrow range of *ca.* 8 ppm (Fig. 3). This was in contrast to AN measurements for chlorometallate ionic liquids, characterised by a single ³¹P NMR signal,⁴⁵ but similar to LCCs, in which multiple Lewis acidic complexes (or multiple potential modes of TEPO coordination) are reflected in several ³¹P NMR signals in AN measurements.³ In all cases, the pattern of signals was the same. There were three high-intensity signals: two relatively sharp and deshielded peaks, and one broader signal shifted upfield by *ca.* 5 ppm, in addition to at least two low intensity peaks. This suggests the existence of several Lewis acidic species capable of interacting with TEPO. The pattern of the ³¹P NMR signals was broadly the same for Ga-SILs and Al-SILs, but the signals for Ga-SILs were deshielded by *ca.* 5 ppm with respect to those for Al-SILs, indicating a stronger interaction of TEPO (higher Lewis acidity) of Ga-SILs.

For the purpose of numerical quantification of Lewis acidity, instead of single AN values, a range of values were reported for each ionic liquid: AN_{Al-SILs} = 70.7–82.7; AN_{Ga-SILs} = 79.6–93.5 (Table 1). On comparing these results with the literature, it can be seen that the Lewis acidity of Al-SILs, $\chi_{Al(OTf)_3} = 0.33$ and 0.25 (AN = 70.8–82.7), was higher than that of 1-octyl-3-methylimidazolium trifluoroaluminate ionic liquids, [C₈mim][OTf]-

Al(OTf)₃, with the same molar ratio of aluminium triflate, $\chi_{Al(OTf)_3} = 0.33$ and 0.25 (AN = 64.9–69.3),¹² but lower than the AN values of archetypal chloroaluminate ionic liquids (AN = 83.3–101.9)^{4,45,47} or AlCl₃ (AN = 85.6–87.0).⁴ The Lewis acidity of Ga-SILs (AN = 79.6–93.5) was higher than that of Al-SILs, approaching the Lewis acidity of chlorogallate ionic liquids [C₈mim]Cl-GaCl₃ with an excess of gallium chloride, $\chi_{GaCl_3} > 0.5$ (AN = 87.7–107.3).⁴ Chlorogallate ionic liquids with a sub-stoichiometric loading of gallium chloride ($\chi_{GaCl_3} = 0.33$) were only mildly acidic, with AN = 21.7.⁴⁵

These results led to two questions: whether the difference in measured AN values translates into a difference in catalytic performance, and how is Lewis acidity related to speciation, considering that in chlorometallate ILs there was a clear and direct link between anionic speciation and AN values.^{4,45}

Speciation of Group 13 SILs

In contrast to Li-based SILs, very little is known about the speciation of Al-based SILs. A single FT-IR spectroscopic study of Al(OTf)₃ and diglyme mixtures, across a range of concentrations: $\chi_{Al(OTf)_3} = 0.286$, 0.130, 0.029 and 0.0015, suggested the presence of free triflate anions in the two most diluted samples, and the prevalence of Al-OTf coordination in the more concentrated samples.³⁵

In this work, speciation of SILs was studied as a function of composition using multinuclear ¹H, ¹³C, ²⁷Al or ⁷¹Ga NMR spectroscopy. All SILs were studied neat; in NMR spectroscopy, a capillary with D₂O was used as a lock and external reference.

The ¹H NMR spectrum of neat triglyme (G3) was compared to the ¹H NMR spectra of G3 : M(OTf)₃ systems (Fig. 4). Signals corresponding to neat glyme, originating from both methylene and methyl groups ($\delta_H = 3.9$ –4.2 ppm), were less shielded than the corresponding signals in SILs ($\delta_H = 3.0$ –3.5 ppm), indicating the coordination of oxygens to the metal centre in SILs.^{48–50} Upon increasing the concentration of M(OTf)₃ in glyme, from $\chi_{M(OTf)_3} = 0.09$ to 0.33, the signals moved gradually

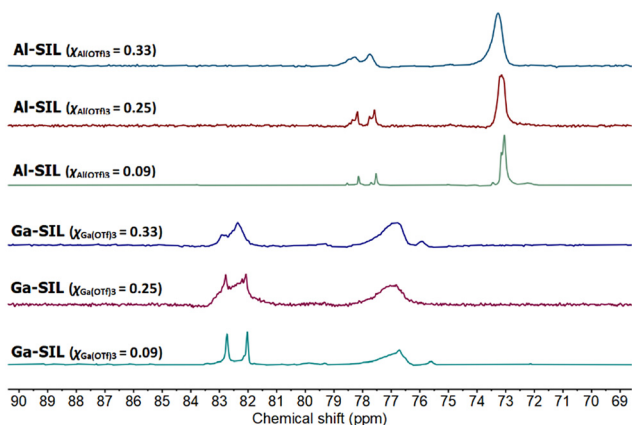


Fig. 3 ³¹P NMR comparison Al-SILs and Ga-SILs, studied across three compositions: $\chi_{M(OTf)_3} = 0.33$, 0.25 and 0.09.

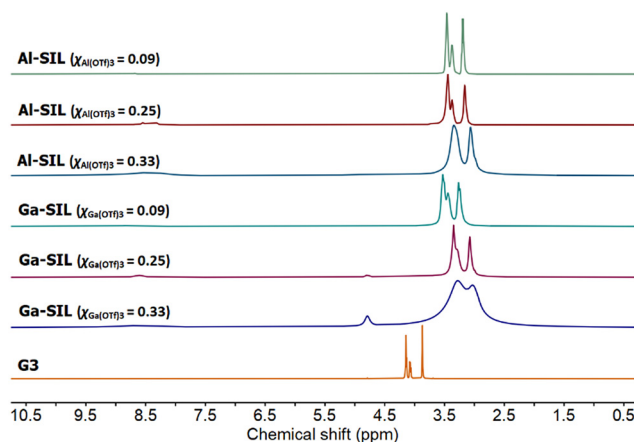


Fig. 4 ¹H NMR spectra of neat glyme, G3, and solvate ionic liquids based on Al(OTf)₃ or Ga(OTf)₃, studied across three compositions: $\chi_{M(OTf)_3} = 0.33$, 0.25 and 0.09.



downfield, as more oxygens were coordinated to aluminium at any given time. Even for very low concentrations of metal salts ($\chi_{\text{M(OTf)}_3} = 0.09$), no signals corresponding to free glyme were visible.

The ^{13}C NMR spectra of neat glyme and selected SILs (Fig. 5) present a slightly different image: in all SILs, the signals corresponding to methylene carbon atoms ($\delta_{^{13}\text{C}} = 66\text{--}72$ ppm) are deshielded when compared to neat glyme ($\delta_{^{13}\text{C}} = 70\text{--}72$ ppm), but no changes are observed for the methyl group signals in neat glyme and in SILs ($\delta_{^{13}\text{C}} = 58$ ppm). The same observation was made by Aldous and co-workers in their study of SILs based on $\text{Li}[\text{NTf}_2]$ and several glymes.⁴⁹ Quartets in the ^{13}C NMR spectra of SILs, arising from CF_3 groups in triflates, are found at $\delta_{^{13}\text{C}} = ca. 119.5$ ppm, which correspond to bound anions.^{51,52}

^{27}Al NMR spectra, recorded for Al-containing SILs (Fig. 6), all featured a group of signals between -13 and 0 ppm corresponding to six-coordinate Al species, in an oxygen coordi-

nation environment.⁵³ Multiple signals suggest the co-existence of several coordination environments of aluminium, in a manner resembling the coordination environment of trifluoroaluminate ionic liquids.¹² There were no signals corresponding to tetrahedral ($40\text{--}140$ ppm), or pentacoordinate ($25\text{--}60$ ppm) aluminium environments,^{54–58} which is unsurprising given the excess of O-donors available in each sample. The very broad signal at *ca.* 75 ppm has been attributed to the residual signal from NMR probe (instrument artefact).¹²

Ga-SILs ($\chi_{\text{Ga(OTf)}_3} = 0.33\text{--}0.09$) were studied by ^{71}Ga NMR spectroscopy (Fig. 7). Most spectra were flat, with signals indistinguishable from the baseline; this is commonly found in gallium-based ionic liquids with low-symmetry anions.⁵⁹ It can be attributed to fast quadrupolar relaxation in these low-symmetry environments, combined with rapid exchanges between several species (as indicated by ^1H NMR spectroscopy), all of which would contribute to the signal broadening. In the most concentrated samples ($\chi_{\text{Ga(OTf)}_3} = 0.33$, 0.25 and possibly 0.20), a signal at -50 ppm was detected, attributable to the octahedral environment of gallium (-50 to 50 ppm).⁶⁰

Finally, both Al-SILs and Ga-SILs were studied by ^{19}F NMR spectroscopy across their entire compositional range ($\chi_{\text{M(OTf)}_3} = 0.33\text{--}0.09$). The ^{19}F NMR spectra of Al-SILs exhibited multiple signals within the chemical shift range of -79.2 to -80.2 ppm (Fig. 8), while ^{19}F NMR signals for Ga-SILs were slightly more shielded on average, -78.9 to -79.6 ppm (Fig. 9). To our knowledge, these are the most complicated patterns of ^{19}F NMR signals from triflate anions reported in the IL literature.

1,3-Dialkylimidazolium ILs with free $[\text{OTf}]^-$ anions, dissolved in a deuterated NMR solvent, all had single sharp ^{19}F NMR signals within -76 to -79 ppm.⁶¹ Al-coordinated triflates in trifluorometallate ILs featured several merged ^{19}F NMR signals, centred around -79 ppm, with minimal downfield shift with increasing $\chi_{\text{Al(OTf)}_3}$, whereas the parent metal-free IL, 1-octyl-3-methylimidazolium triflate, measured neat, had a singlet at -80.2 ppm.¹²

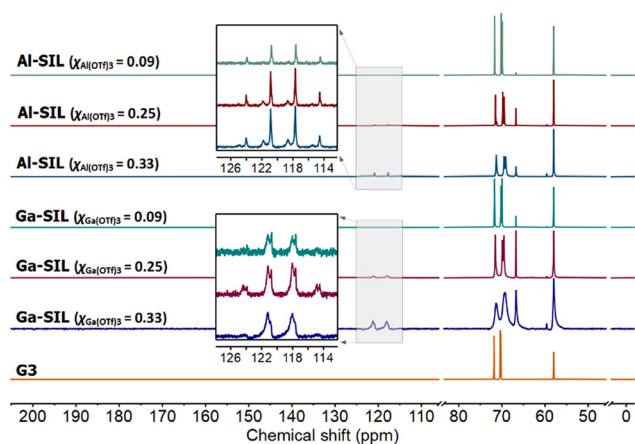


Fig. 5 ^{13}C NMR spectra of neat glyme, G3, and solvate ionic liquids based on Al(OTf)_3 or Ga(OTf)_3 , studied across three compositions: $\chi_{\text{M(OTf)}_3} = 0.33$, 0.25 and 0.09.

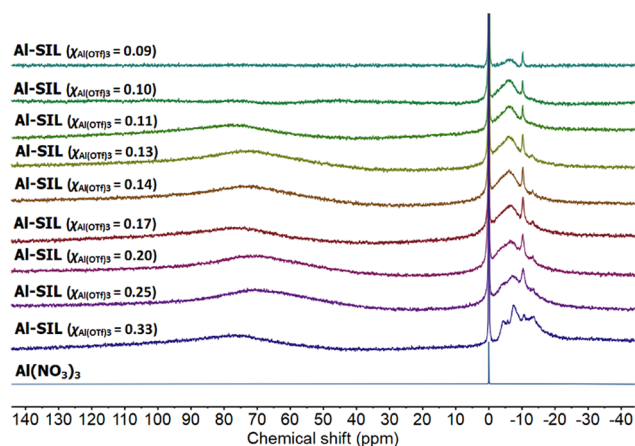


Fig. 6 ^{27}Al NMR spectra of $\text{Al(NO}_3)_3$ in D_2O , and a full series of Al-SIL compositions, $\chi_{\text{Al(OTf)}_3} = 0.33\text{--}0.09$.

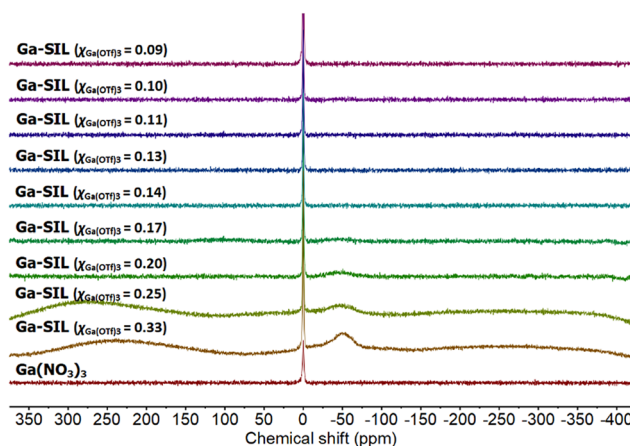


Fig. 7 ^{71}Ga NMR spectrum of $\text{Ga(NO}_3)_3$ in D_2O and a full series of Ga-SIL compositions, $\chi_{\text{Ga(OTf)}_3} = 0.33\text{--}0.09$.



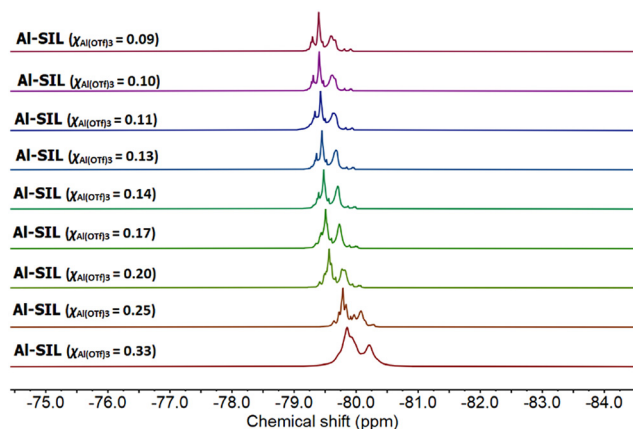


Fig. 8 ^{19}F NMR spectra of a full series of Al-SILs, $\chi_{\text{Al}(\text{OTf})_3} = 0.33\text{--}0.09$.

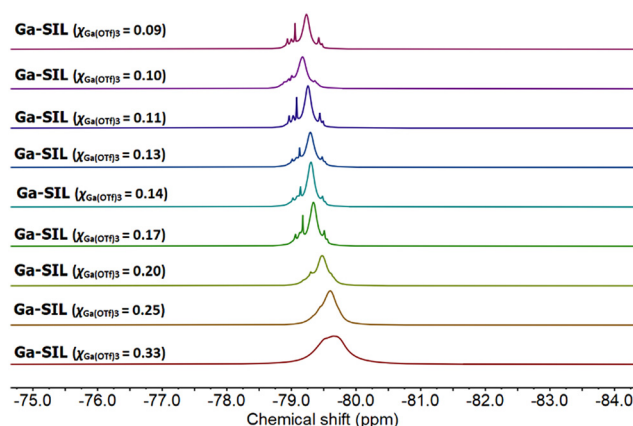


Fig. 9 ^{19}F NMR spectra of a full series of Ga-SILs, $\chi_{\text{Ga}(\text{OTf})_3} = 0.33\text{--}0.09$.

In this work, all ^{19}F NMR signals shifted upfield with increasing $\chi_{\text{M}(\text{OTf})_3}$, although the pattern of signals did not change significantly with the composition (aside from broadening due to viscosity change). It is understood that speciation of the metal remains constant across the compositional range (hence the pattern of signals remains constant), but their solvent environment changes (hence the solvent-induced change in the chemical shift). Namely, at $\chi_{\text{M}(\text{OTf})_3} = 0.33$, the neat sample is the neat solvate ionic liquid, composed of Al or Ga coordinated by glymes and triflate anions – a “good” SIL, with strong coulombic interactions. In the neat $\chi_{\text{M}(\text{OTf})_3} = 0.09$ composition, there are the same triflate anions, and the same coordination complexes of Al or Ga, but they are diluted with excess glyme, acting as a solvent. This change of solvent, from a neat ionic liquid to a solution of ionic liquid in glyme, results in a change in the chemical shift. In both Al-SILs and Ga-SILs, this transition from solution to the SIL environment is observable for $\chi_{\text{M}(\text{OTf})_3} \geq 0.20$.

In conclusion, NMR spectroscopy points to both aluminium and gallium having octahedral coordination, with both $[\text{OTf}]^-$ and G3 ligands coordinated to the metal centre. It can be certainly stated that there is no single well-defined

species in any sample, but there are multiple octahedral complexes, each characterised by a number of $[\text{OTf}]^-$ anions and specific numbers/hapticities of G3 ligands around the metal centre.

On comparing the ^{19}F NMR spectra of Al-SILs (Fig. 8) and Ga-SILs (Fig. 9), further conclusions could be cautiously proposed. Firstly, although there are multiple species, both in Al-SIL and in Ga-SIL, they do not seem to change as a function of $\chi_{\text{M}(\text{OTf})_3}$ in either system. Rather, it could be envisaged that the $\chi_{\text{M}(\text{OTf})_3} = 0.33$ composition is the concentrated SIL and adding more glyme (towards $\chi_{\text{M}(\text{OTf})_3} = 0.09$) dilutes the metal species without affecting their coordination environments. AN measurements corroborate this hypothesis, as the range of AN values appears constant for each family of SILs (Table 1). Secondly, the ^{19}F NMR spectra of Al-SILs and Ga-SILs are markedly different; there seems to be an additional deshielded signal in the Al-SIL spectra, which reaches -80.2 ppm for $\chi_{\text{Al}(\text{OTf})_3} = 0.33$ (more ionic nature, *viz.* Fig. 2b). In Ga-SILs, all triflates appear to be bound, suggesting that the equilibrium in Fig. 2b is right-shifted for gallium.

Notably, in all samples, there is an excess of O-donors with respect to metal centres. Although no free glymes were detected by ^1H or ^{13}C NMR spectroscopy, it must be assumed that dynamic exchange of glyme ligands occurs.

Thermogravimetric analysis

The thermal stability of the solvate ionic liquids was studied by thermogravimetric analysis (TGA). TG curves are available in Fig. S1 and S2 in the ESI.† In contrast to their thermally stable precursors, glyme ($T_d = 167$ °C), $\text{Al}(\text{OTf})_3$ ($T_d = 221$ °C) and $\text{Ga}(\text{OTf})_3$ ($T_d = 182$ °C), the thermal stability of the investigated systems was much lower with $T_{d5\%} = 127$ °C for Al-SILs and $T_{d5\%} = 105$ °C Ga-SILs, respectively. This unfortunately limits the span of operative conditions for these glymes, but also suggests that the metal centre is highly Lewis acidic, effectively catalysing the decomposition of the glyme at a much lower temperature.

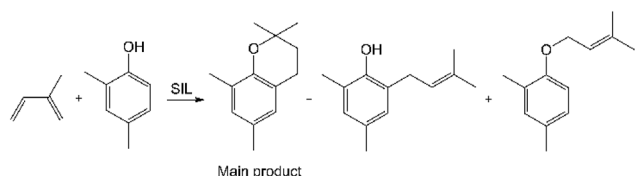
Catalytic performance in a [3 + 3] cycloaddition reaction

A [3 + 3] cycloaddition was selected as a test reaction for the catalytic activity of the new SILs. The yield and selectivity of products in this reaction depend strongly both on the activity of the Lewis acidic catalyst and on the reaction conditions, which makes it sensitive to subtle changes and therefore a good model to distinguish between catalysts.^{62,63}

The synthesis of chromane from 2,4-dimethylphenol and isoprene (Scheme 1) was chosen as a model [3 + 3] cycloaddition. Chromane is a part of a structure of more complicated compounds, including various forms of vitamin E and flavonoids,⁶⁴ which makes it a common synthetic target. The reaction is typically catalysed by metal triflates, promoting high selectivity towards chromane (main product, Scheme 1).⁶⁵

All reactions were carried out solventless, at 35 °C, using liquid reactants (1 : 2 molar ratio of isoprene : 2,4-dimethylphenol). Conversion of 2,4-dimethylphenol was monitored using GC, and each reaction was carried out until a plateau of





Scheme 1 Reaction between 2,4-dimethylphenol and isoprene.

conversion was reached. All SILs formed homogeneous solutions when added to the reaction mixture, whereas their corresponding solid metal triflates, studied as comparators, were suspended in the reaction mixture.

The catalytic performance of $\text{Al}(\text{OTf})_3$, at 2 mol% loading of aluminium with respect to isoprene, was compared to Al-SIL ($\chi_{\text{Al}(\text{OTf})_3} = 0.33$), at 1, 2 and 5 mol% (Fig. 10). While the conversion for 2 mol% of $\text{Al}(\text{OTf})_3$ reached a plateau at *ca.* 70%, the same loading of Al-SIL ($\chi_{\text{Al}(\text{OTf})_3} = 0.33$) gave *ca.* 99% conversion after 240 min, with the same selectivity to chromane of *ca.* 80%. Increasing the Al-SIL loading to 5 mol% resulted in improved reaction kinetics and selectivity; it gave full substrate conversion within 120 min, with selectivity reaching a maximum of 90.7% after 180 min. Decreasing the Al-SIL loading to 1 mol% had the opposite effect, with performance lower than that of the benchmark catalyst, *i.e.* 2 mol% of $\text{Al}(\text{OTf})_3$.

In a series of analogous experiments, the performance of $\text{Ga}(\text{OTf})_3$, at 2 mol% loading, was compared to Ga-SIL ($\chi_{\text{Ga}(\text{OTf})_3} = 0.33$), at 1, 2 and 5 mol% loadings (Fig. 11). The reaction catalysed with 2 mol% of $\text{Ga}(\text{OTf})_3$ reached *ca.* 91% conversion after 240 min, with selectivity approaching 90%, whereas the same loading of Ga-SIL ($\chi_{\text{Ga}(\text{OTf})_3} = 0.33$) gave full conversion

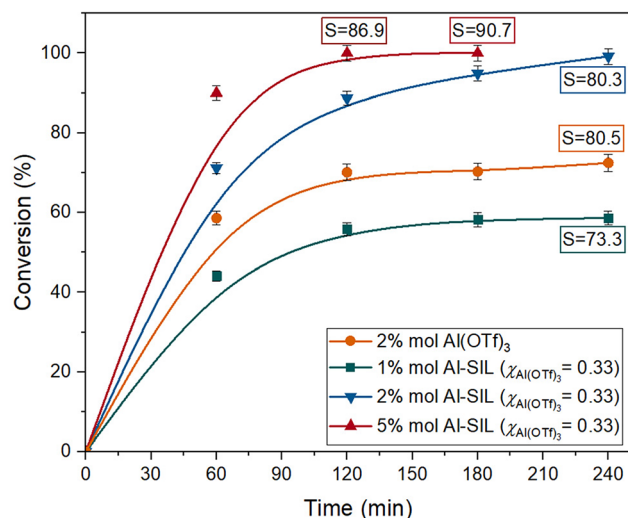


Fig. 10 Performance of various amounts of Al-SIL ($\chi_{\text{Al}(\text{OTf})_3} = 0.33$) in the [3 + 3] cycloaddition of 2,4-dimethylphenol to isoprene, relative to metal triflate. Reaction conditions: 2,4-dimethylphenol (8 mmol), isoprene (4 mmol), 1000 rpm, $T = 35^\circ\text{C}$, S – selectivity to the main product.

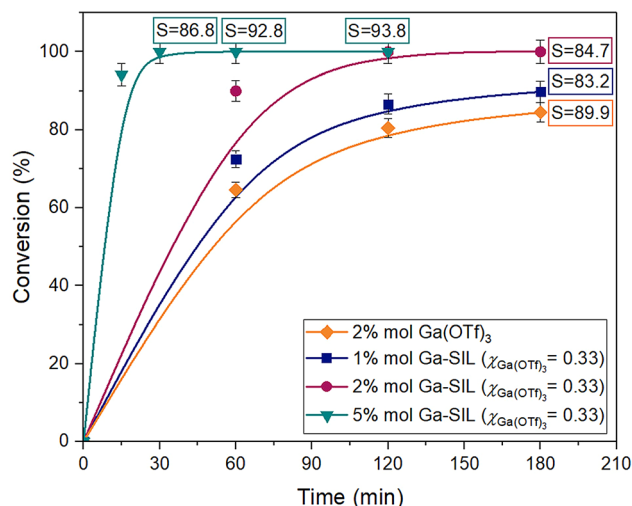


Fig. 11 Performance of various amounts of Ga-SIL ($\chi_{\text{Ga}(\text{OTf})_3} = 0.33$) in the [3 + 3] cycloaddition of 2,4-dimethylphenol to isoprene, relative to metal triflate. Reaction conditions: 2,4-dimethylphenol (8 mmol), isoprene (4 mmol), 1000 rpm, $T = 35^\circ\text{C}$, S – selectivity to the main product.

after only 30 min. The extended reaction time increased the selectivity, from 86.8% after 30 min to 93.8% after 120 min.

Both gallium triflate and Ga-SIL significantly outperformed their aluminium-based analogues, in keeping with higher AN values recorded for Ga-SIL (Table 1). The Ga-SIL ($\chi_{\text{Ga}(\text{OTf})_3} = 0.33$, loading 2 mol%) gave full conversion in 120 min, whereas the analogous Al-SIL required 240 min.

The best outcomes, in terms of conversion and selectivity, achieved with each tested catalyst, are given in Table 2, along with the corresponding experimental conditions. Both Al-SIL and Ga-SIL outperformed their corresponding triflates at the same loadings of 2 mol%. Inferior reaction rates in $\text{M}(\text{OTf})_3$ -catalysed reactions could be attributed to poor mass transport, as the triflate salts were suspended rather than dissolved. However, for both $\text{M}(\text{OTf})_3$ catalysts, conversions reached plateau values, whereas SILs enabled both full conversions and higher selectivities to chromane, which cannot be attributed solely to mass transfer. We therefore concluded that altering coordination around the metal centres, from triflate-only to mixed glyme/triflate complexes, had the dual benefit of (i) increased solubility in the organic phase and (ii) increased catalytic activity.

Following this reasoning, it was concluded that further altering of the coordination environment of Al(III) and Ga(III), from triflate to glyme ligands, could be beneficial. To test this hypothesis, both SILs were tested at $\chi_{\text{M}(\text{OTf})_3} = 0.09$, with a vastly increased concentration of G3 with respect to metal. However, even at 5 mol% loading, the $\chi_{\text{M}(\text{OTf})_3} = 0.09$ SILs produced inferior results (Table 2, entries 4 and 8), when compared to $\chi_{\text{M}(\text{OTf})_3} = 0.33$ SILs (Table 2, entries 2, 3, 6 and 7). Most likely, liquids at $\chi_{\text{M}(\text{OTf})_3} = 0.09$ are merely solutions of SILs of certain fixed compositions in the excess of glyme; upon addition to the reaction mixture, excess glyme is simply

Table 2 Performance of SILs in the [3 + 3] cycloaddition of 2,4-dimethylphenol to isoprene

No.	Catalyst	$\chi_{\text{M(OTf)}_3}$	Catalyst loading (mol%)	Time (min)	Conversion (%)	Selectivity (%)
1	Al(OTf) ₃	1.00	2	180	70.3	80.3
2	Al-SIL	0.33	2	240	99.2	80.3
3	Al-SIL	0.33	5	180	100.0	90.7
4	Al-SIL	0.09	5	240	64.0	70.9
5	Ga(OTf) ₃	1.00	2	240	91.4	83.2
6	Ga-SIL	0.33	2	120	100.0	82.8
7	Ga-SIL	0.33	5	120	100.0	93.8
8	Ga-SIL	0.09	5	240	92.6	84.3

Reaction conditions: 2,4-dimethylphenol (8 mmol), isoprene (4 mmol), 1000 rpm, $T = 35^\circ\text{C}$, amount of catalyst calculated in relation to isoprene.

Table 3 Recycling of Ga-SIL ($\chi_{\text{Ga(OTf)}_3} = 0.33$) in the [3 + 3] cycloaddition of 2,4-dimethylphenol to isoprene

Cycle no.	Conversion (%)	Selectivity (%)
1	100.0	93.8
2	100.0	94.0
3	100.0	92.6
4	100.0	91.5

Reaction conditions: 2,4-dimethylphenol (12–16 mmol), isoprene (6–8 mmol), 1000 rpm, $T = 35^\circ\text{C}$, 5 mol% of Ga-SIL ($\chi_{\text{Ga(OTf)}_3} = 0.33$) (amount of catalyst calculated in relation to isoprene), 120 min.

washed away and acts as a dilutant to the system, decreasing the overall concentration of reactants.

The recyclability of the best-performing SIL, Ga-SIL ($\chi_{\text{Ga(OTf)}_3} = 0.33$), was tested by extracting the residual substrate and product with anhydrous hexane, after which the phase-separated catalyst layer was isolated, washed twice with hexene, concentrated and used in the next reaction cycle. Full conversion of the substrate was achieved over 4 consecutive reaction cycles, with selectivities above 90% (Table 3).

In conclusion, the G3:Ga(OTf)₃, $\chi_{\text{Ga(OTf)}_3} = 0.33$ SIL was found to be an excellent catalyst for the synthesis of chromane, giving full conversion of isoprene within 2 h, with selectivity towards 2,2-dimethyl-6,8-dimethylchromane reaching 93.8%, slightly higher than those of previously reported catalytic systems, ranging from 80% to 92%.^{12,66,67} The catalytic performance of Al-SILs and Ga-SILs has followed the AN trend.

Conclusions

New solvate ionic liquids based on aluminium(III) and gallium(III) triflates, and G3 have been synthesised, characterised and used as Lewis acidic catalysts for the synthesis of chromane. Both triflate salts dissolved in G3 at low concentrations ($\chi_{\text{M(OTf)}_3} = 0.09$) and formed homogeneous liquids up to a metal triflate loading of $\chi_{\text{M(OTf)}_3} = 0.33$. It was found that both metals were octahedral across the entire compositional range,

and both G3 and [OTf][−] were included in the first coordination sphere of the metal.

From multinuclear NMR spectroscopic experiments, it appeared that the coordination environment remained similar across the compositional range, for each of the two metals. Furthermore, it was suggested that speciation of Al-SILs was different from that of Ga-SILs, potentially with more free triflate in the former. AN values (an experimental measure of Lewis acidity) were constant for each SIL family, across the entire compositional range: *ca.* 71–83 for Al-SILs and *ca.* 80–93 for Ga-SILs. These values lie within a relatively high acidity range, despite a fully occupied coordination shell.

The catalytic activity of SILs was tested in a model [3 + 3] cycloaddition, yielding 2,2-dimethyl-2,4-dimethylchromane. Both families of SILs were fully dissolved in the reaction mixtures, in contrast to the parent metal triflates, and their catalytic activity has been enhanced when compared at the same metal loading. The catalytic performance was aligned with AN measurements, with Ga-SILs outperforming Al-SILs. The best catalyst (Ga-SIL $\chi_{\text{M(OTf)}_3} = 0.33$) gave full substrate conversion and a high selectivity of 93.8% after 2 h at 35 °C, and could be recycled four times, retaining consistently high conversion and selectivity.

Given the notorious difficulties in dissolving metal triflates, converting them to SILs may offer a broadly-applicable and robust approach to generate well-soluble metal triflate catalysts; this strategy is likely applicable beyond Group 13, to rare earth triflates and transition metal triflates. Further detailed studies on the structure and applications of Group 13 SILs are currently ongoing in our group.

Author contributions

Justyna Więclawik: data curation, formal analysis, investigation, methodology, validation, visualization and writing – original draft; Alina Brzeczek-Szafran: conceptualisation, formal analysis, methodology, visualization, writing – original draft, and writing – review & editing; Sebastian Jurczyk: formal analysis and methodology; Karolina Matuszek: methodology, validation, and writing – review & editing; Małgorzata Swadźba-Kwaśny: conceptualisation, funding acquisition, supervision, writing – original draft, and writing – review & editing; Anna Chrobok: conceptualisation, funding acquisition, supervision, writing – original draft, and writing – review & editing.

Data availability

The data supporting this article have been included as part of the ESI.†

Conflicts of interest

There are no conflicts to declare.



Acknowledgements

The financial support from the National Science Centre, Poland (grant no. UMO-2020/39/B/ST8/00693) is gratefully acknowledged. The authors also express gratitude to the Polish National Agency for Academic Exchange (under the Academic International Partnerships Program, grant agreement PPI/APM/2018/1/00004) for financial support of the internship at The QUILL Research Centre, Queen's University Belfast, which enabled a part of the speciation study, the Polish National Agency for Academic Exchange and grant agreement BPI/PST/2021/1/00039 for enabling scientific discussions in a project funded within the Strategic Partnerships program that helped us interpret a phenomenon described above.

Notes and references

- 1 C. A. Angell, *J. Electrochem. Soc.*, 1965, **112**, 1224.
- 2 C. Austen Angell, Y. Ansari and Z. Zhao, *Faraday Discuss.*, 2012, **154**, 9–27.
- 3 F. Coleman, G. Srinivasan and M. Swadźba-Kwaśny, *Angew. Chem., Int. Ed.*, 2013, **52**, 12582–12586.
- 4 J. M. Hogg, L. C. Brown, K. Matuszek, P. Latos, A. Chrobok and M. Swadźba-Kwaśny, *Dalton Trans.*, 2017, **46**, 11561–11574.
- 5 J. M. Hogg, F. Coleman, A. Ferrer-Ugalde, M. P. Atkins and M. Swadźba-Kwaśny, *Green Chem.*, 2015, **17**, 1831–1841.
- 6 K. Matuszek, A. Chrobok, J. M. Hogg, F. Coleman and M. Swadźba-Kwaśny, *Green Chem.*, 2015, **17**, 4255–4262.
- 7 M. Lijewski, J. M. Hogg, M. Swadźba-Kwaśny, P. Wasserscheid and M. Haumann, *RSC Adv.*, 2017, **7**, 27558–27563.
- 8 S. Kobayashi, M. Sugiura, H. Kitagawa and W. W. L. Lam, *Chem. Rev.*, 2002, **102**, 2227–2302.
- 9 L. Massi, J. F. Gal and E. Duñach, *ChemPlusChem*, 2022, **87**, e202200037.
- 10 G. A. Olah, O. Farooq, S. M. F. Farnia and J. A. Olah, *J. Am. Chem. Soc.*, 1988, **110**, 2560–2565.
- 11 M. Distaso and E. Quaranta, *Tetrahedron*, 2004, **60**, 1531–1539.
- 12 P. Latos, A. Culkin, N. Barteczko, S. Boncel, S. Jurczyk, L. C. Brown, P. Nockemann, A. Chrobok and M. Swadźba-Kwaśny, *Front. Chem.*, 2018, **6**, 1–15.
- 13 T. Tamura, T. Hachida, K. Yoshida, N. Tachikawa, K. Dokko and M. Watanabe, *J. Power Sources*, 2010, **195**, 6095–6100.
- 14 T. Mandai, K. Yoshida, K. Ueno, K. Dokko and M. Watanabe, *Phys. Chem. Chem. Phys.*, 2014, **16**, 8761–8772.
- 15 T. Mandai, K. Yoshida, S. Tsuzuki, R. Nozawa, H. Masu, K. Ueno, K. Dokko and M. Watanabe, *J. Phys. Chem. B*, 2015, **119**, 1523–1534.
- 16 T. Tamura, K. Yoshida, T. Hachida, M. Tsuchiya, M. Nakamura, Y. Kazue, N. Tachikawa, K. Dokko and M. Watanabe, *Chem. Lett.*, 2010, **39**, 753–755.
- 17 C. Zhang, K. Ueno, A. Yamazaki, K. Yoshida, H. Moon, T. Mandai, Y. Umabayashi, K. Dokko and M. Watanabe, *J. Phys. Chem. B*, 2014, **118**, 5144–5153.
- 18 C. Zhang, A. Yamazaki, J. Murai, J. W. Park, T. Mandai, K. Ueno, K. Dokko and M. Watanabe, *J. Phys. Chem. C*, 2014, **118**, 17362–17373.
- 19 H. Hirayama, N. Tachikawa, K. Yoshii, M. Watanabe and Y. Katayama, *Electrochemistry*, 2015, **83**, 824–827.
- 20 K. Ueno, J. Murai, K. Ikeda, S. Tsuzuki, M. Tsuchiya, R. Tatara, T. Mandai, Y. Umabayashi, K. Dokko and M. Watanabe, *J. Phys. Chem. C*, 2016, **120**, 15792–15802.
- 21 M. Watanabe, K. Dokko, K. Ueno and M. L. Thomas, *Bull. Chem. Soc. Jpn.*, 2018, **91**, 1660–1682.
- 22 Z. Yu, C. Fang, J. Huang, B. G. Sumpter and R. Qiao, *ACS Appl. Mater. Interfaces*, 2018, **10**, 32151–32161.
- 23 S. Terada, K. Ikeda, K. Ueno, K. Dokko and M. Watanabe, *Aust. J. Chem.*, 2019, **72**, 70–80.
- 24 S. Wei, Z. Li, K. Kimura, S. Inoue, L. Pandini, D. Di Lecce, Y. Tominaga and J. Hassoun, *Electrochim. Acta*, 2019, **306**, 85–95.
- 25 D. J. Eyckens and L. C. Henderson, *Front. Chem.*, 2019, **7**, 1–15.
- 26 D. J. Eyckens, M. E. Champion, B. L. Fox, P. Yoganantharajah, Y. Gibert, T. Welton and L. C. Henderson, *Eur. J. Org. Chem.*, 2016, **2016**, 913–917.
- 27 A. Obregón-Zúñiga, M. Milán and E. Juaristi, *Org. Lett.*, 2017, **19**, 1108–1111.
- 28 D. J. Eyckens and L. C. Henderson, *RSC Adv.*, 2017, **7**, 27900–27904.
- 29 S. Di Pietro, V. Bordoni, A. Mezzetta, C. Chiappe, G. Signore, L. Guazzelli and V. Di Bussolo, *Molecules*, 2019, **24**, 1–9.
- 30 N. Hameed, D. J. Eyckens, B. M. Long, N. V. Salim, J. C. Capricho, L. Servinis, M. De Souza, M. D. Perus, R. J. Varley and L. C. Henderson, *ACS Appl. Polym. Mater.*, 2020, **2**, 2651–2657.
- 31 T. Mandai, K. Dokko and M. Watanabe, *Chem. Rec.*, 2019, **19**, 708–722.
- 32 Z. Ma, M. Forsyth, D. R. MacFarlane and M. Kar, *Green Energy Environ.*, 2019, **4**, 146–153.
- 33 K. Matuszek, A. Chrobok, F. Coleman, K. R. Seddon and M. Swadźba-Kwaśny, *Green Chem.*, 2014, **16**, 3463–3471.
- 34 A. Brzęczek-Szafran, J. Więclawik, N. Barteczko, A. Szelwicka, E. Byrne, A. Kolanowska, M. Swadźba-Kwaśny and A. Chrobok, *Green Chem.*, 2021, **23**, 4421–4429.
- 35 L. D. Reed, A. Arteaga and E. J. Menke, *J. Phys. Chem. B*, 2015, **119**, 12677–12681.
- 36 L. D. Reed, S. N. Ortiz, M. Xiong and E. J. Menke, *Chem. Commun.*, 2015, **51**, 14397–14400.
- 37 S. Gu, Y. Haoyi, Y. Yuan, Y. Gao, N. Zhu, F. Wu, Y. Bai and C. Wu, *Energy Mater. Adv.*, 2022, **1**, 1–10.
- 38 A. Kitada, K. Nakamura, K. Fukami and K. Murase, *Electrochemistry*, 2014, **82**, 946–948.
- 39 A. Kitada, K. Nakamura, K. Fukami and K. Murase, *Electrochim. Acta*, 2016, **211**, 561–567.



- 40 Z. Zhang, A. Kitada, S. Gao, K. Fukami, N. Tsuji, Z. Yao and K. Murase, *ACS Appl. Mater. Interfaces*, 2020, **12**, 43289–43298.
- 41 A. R. Jupp, T. C. Johnstone and D. W. Stephan, *Dalton Trans.*, 2018, **47**, 7029–7035.
- 42 P. Erdmann, J. Leitner, J. Schwarz and L. Greb, *ChemPhysChem*, 2020, **21**, 987–994.
- 43 J. Estager, P. Nockemann, K. R. Seddon, M. Swadźba-Kwaśny and S. Tyrrell, *Inorg. Chem.*, 2011, **50**, 5258–5271.
- 44 M. Currie, J. Estager, P. Licence, S. Men, P. Nockemann, K. R. Seddon, M. Swadźba-Kwaśny and C. Terrade, *Inorg. Chem.*, 2013, **52**, 1710–1721.
- 45 J. Estager, A. A. Oliferenko, K. R. Seddon and M. Swadźba-Kwaśny, *Dalton Trans.*, 2010, **39**, 11375–11382.
- 46 K. Matuszek, S. Coffie, A. Chrobok and M. Swadźba-Kwaśny, *Catal. Sci. Technol.*, 2017, **7**, 1045–1049.
- 47 M. Sakhalakar, R. P. Choudhury, V. Bhakthavatsalam, S. V. Lande, J. Pradhan and S. Chandra, *J. Mol. Struct.*, 2020, **1222**, 128936.
- 48 N. Peddagopu, P. Rossi, C. Bonaccorso, A. Bartasyte, P. Paoli and G. Malandrino, *Dalton Trans.*, 2020, **49**, 1002–1006.
- 49 J. J. Black, A. Dolan, J. B. Harper and L. Aldous, *Phys. Chem. Chem. Phys.*, 2018, **20**, 16558–16567.
- 50 S. Sun, Y. Niu, Q. Xu, Z. Sun and X. Wei, *RSC Adv.*, 2015, **5**, 46564–46567.
- 51 L. L. Tolstikova, A. V. Bel'Skikh and B. A. Shainyan, *Russ. J. Org. Chem.*, 2010, **46**, 383–388.
- 52 P. Latos, A. Wolny, J. Zdarta, F. Ciesielczyk, S. Jurczyk, T. Jesionowski and A. Chrobok, *Environ. Technol. Innovation*, 2023, **31**, 103164.
- 53 M. M. Finnegan, S. J. Rettig and C. Orvig, *J. Am. Chem. Soc.*, 1986, **108**, 5033–5035.
- 54 G. A. Olah, O. Farooq, S. M. F. Farnia, M. R. Bruce, F. L. Clouet, P. R. Morton, G. K. S. Prakash, R. C. Stevens, R. Bau, K. Lammertsma, S. Suzer and L. Andrews, *J. Am. Chem. Soc.*, 1988, **110**, 3231–3238.
- 55 D. A. Atwood, *Coord. Chem. Rev.*, 1998, **176**, 407–430.
- 56 M. Choi, K. Matsunaga, F. Oba and I. Tanaka, *J. Phys. Chem. C*, 2009, **113**, 3869–3873.
- 57 A. W. Apblett, in *Encyclopedia of Inorganic and Bioinorganic Chemistry*, John Wiley & Sons, Ltd, 2012.
- 58 K. N. Tayade, M. Mishra, K. Munusamy and R. S. Somani, *Catal. Sci. Technol.*, 2015, **5**, 2427–2440.
- 59 K. R. Seddon, G. Srinivasan, M. Swadźba-Kwaśny and A. R. Wilson, *Phys. Chem. Chem. Phys.*, 2013, **15**, 4518–4526.
- 60 Z. L. Ma, K. M. Wentz, B. A. Hammann, I. Y. Chang, M. K. Kamunde-Devonish, P. H. Y. Cheong, D. W. Johnson, V. V. Terskikh and S. E. Hayes, *Chem. Mater.*, 2014, **26**, 4978–4983.
- 61 N. V. Ignat'ev, P. Barthen, A. Kucheryna, H. Willner and P. Sartori, *Molecules*, 2012, **17**, 5319–5338.
- 62 P. Quadrelli, *Modern applications of cycloaddition chemistry*, Elsevier, 2019.
- 63 J. Deng, X. N. Wang and R. P. Hsung, in *Wiley Blackwell 6*, Wiley Blackwell, 2014, vol. 9781118299, pp. 283–354.
- 64 C. Schneider, *Mol. Nutr. Food Res.*, 2005, **49**, 7–30.
- 65 S. W. Youn and J. I. Eom, *J. Org. Chem.*, 2006, **71**, 6705–6707.
- 66 Y. Yamamoto and K. Itonaga, *Org. Lett.*, 2009, **11**, 717–720.
- 67 T. T. Dang, F. Boeck and L. Hintermann, *J. Org. Chem.*, 2011, **76**, 9353–9361.

